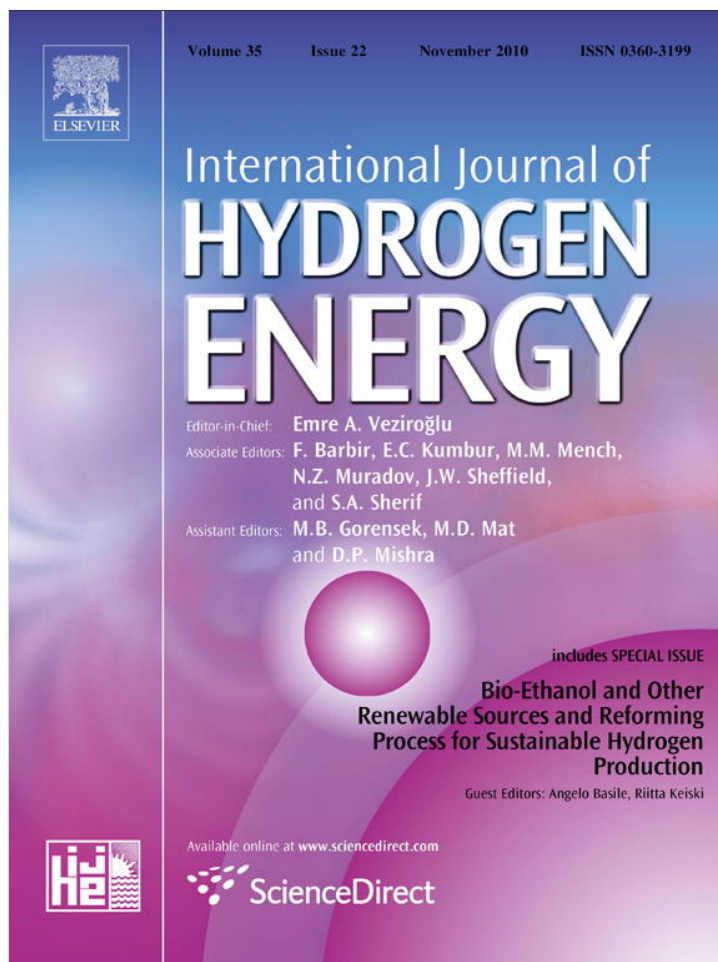


Provided for non-commercial research and education use.
Not for reproduction, distribution or commercial use.

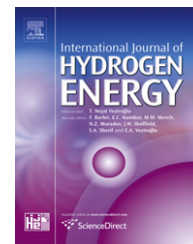


This article appeared in a journal published by Elsevier. The attached copy is furnished to the author for internal non-commercial research and education use, including for instruction at the authors institution and sharing with colleagues.

Other uses, including reproduction and distribution, or selling or licensing copies, or posting to personal, institutional or third party websites are prohibited.

In most cases authors are permitted to post their version of the article (e.g. in Word or Tex form) to their personal website or institutional repository. Authors requiring further information regarding Elsevier's archiving and manuscript policies are encouraged to visit:

<http://www.elsevier.com/copyright>

Available at www.sciencedirect.comjournal homepage: www.elsevier.com/locate/he

Analysis of trace impurities in hydrogen: Enrichment of impurities using a H₂ selective permeation membrane[☆]

Shabbir Ahmed, Sheldon H.D. Lee, Dionissios D. Papadias*

Argonne National Laboratory, Chemical Sciences and Engineering Division, 9700 S. Cass Avenue, Lemont, IL 60439, USA

ARTICLE INFO

Article history:

Received 28 June 2010

Received in revised form

11 August 2010

Accepted 11 August 2010

Available online 15 September 2010

Keywords:

Hydrogen quality

Trace contaminants

Analytical methods

Impurity enrichment

Dense metal membrane

ABSTRACT

A laboratory-scale gas sampling and impurity enrichment device (GSIED) using a Pd/Cu-coated Pd–Ag alloy hydrogen selective permeation membrane has been designed, fabricated, and tested to show that such a device provides an effective method to enrich trace impurity species in hydrogen by factors of 10–100 or greater. The enrichment process will allow analysis of these impurities in hydrogen using simpler and less expensive analytical instruments that can be deployed in the fields. A series of experiments was conducted with the device using a hydrogen analyte gas containing N₂, CH₄, and CO₂ at ~0.1% each, CO at ~100 ppm, and H₂S at ~2 ppm. Chemical analyses of the impurity-enriched sample showed that for the non-sulfur species, the measured enrichment factors were 14.5–14.9, which closely matched the calculated enrichment factors of 14.8–14.9. The elemental material balances indicated a good accounting of the non-sulfur impurity species. For the sulfur species, some initial sulfur loss was observed, presumably due to interaction with the surfaces and/or analytical deficiencies. The impurity enrichment factors for such sampling devices are functions of the sampler size, and the sample vessel pressures before and after enrichment. Depending on the volume of the enriched sample needed for analysis, the device can be designed to enrich the impurities in hydrogen by more than a factor of two orders of magnitude for practical and economical field applications.

© 2010 Professor T. Nejat Veziroglu. Published by Elsevier Ltd. All rights reserved.

1. Introduction

Fuel cell and other hydrogen fueled vehicles are slated for commercial deployment in the US and around the world in the near future. A number of demonstration hydrogen refueling centers have been set up around the US. Several teams of vehicle manufacturers and fuel suppliers have worked with state and federal governments and other organizations to demonstrate

hydrogen refueling centers [1–3], where the hydrogen is dispensed into the vehicle's tanks at up to ~680 atm (10,000 psig). Since fuel cells are very sensitive to certain impurities, such as carbon monoxide, hydrogen sulfide, and ammonia, the fuel supplier must ensure that the concentrations of such species in the dispensed hydrogen are within acceptable limits.

Several organizations, such as ISO and SAE International, are working to establish allowable impurity levels in fuel H₂

Abbreviations and acronyms: ASTM, American Society for Testing and Materials; CEF, calculated enrichment factor; EF, enrichment factor; ISO, International Organization for Standardization; MEF, measured enrichment factor; SAE, Society of Automotive Engineers; GSIED, gas sampling and impurity enrichment device.

[☆] The U.S. Government retains for itself, and others acting on its behalf, a paid-up, nonexclusive, irrevocable worldwide license in said article to reproduce, prepare derivative works, distribute copies to the public and perform publicly and display publicly, by or on behalf of the Government.

* Corresponding author. Tel.: +1 630 252 3206.

E-mail address: papadias@anl.gov (D.D. Papadias).

0360-3199/\$ – see front matter © 2010 Professor T. Nejat Veziroglu. Published by Elsevier Ltd. All rights reserved.

doi:10.1016/j.ijhydene.2010.08.042

| Notation | | Sub- and superscripts | |
|-----------|--|-----------------------|----------------------------------|
| C | concentration, mol/m ³ | 0 | inlet properties, analyte gas |
| K | membrane permeability constant, mol/s, Pa ^{0.5} | 1 | sampling vessel |
| \dot{n} | molar flow-rate, mol/s | 2 | impurity enrichment vessel |
| n | molar mass, mol | i | impurity species |
| P | pressure, Pa | I | total amount of impurity species |
| R | specific gas constant, J/(mol K) | T | total amount of gas |
| T | temperature, K | amb | ambient |
| V | volume, m ³ | hi | high |
| y | molar fraction, – | lo | low |
| Z | compressibility factor, – | | |

for fuel cell powered vehicles. The guideline values for some of the key impurities proposed in the SAE International's Surface Vehicle Information Report are shown in Table 1 [4]. The table shows that the limits on CO, NH₃ and sulfur are extremely low and are at or even below the detection limits of standardized analytical methods. Organizations such as the ASTM¹ are developing new standardized methods for the analysis of impurities in hydrogen for fuel cells.

The current practice at demonstration hydrogen refueling stations is to take grab samples periodically and send the samples to specialty laboratories for analysis using state-of-the-art instruments, such as, for example, a gas chromatograph fitted with a pulse discharged helium ionization detector (GC/PDHID) to analyze for carbon monoxide at concentrations of 0.2 parts per million or lower, or a gas chromatograph fitted with a sulfur chemiluminescence detector (GC/SCD) to analyze for total sulfur species. These sensitive instruments are expensive, and they require considerable laboratory time of skilled analytical chemists to operate and maintain them.

With the larger deployment of fuel cell vehicles and the anticipated growth in the refueling infrastructure in the years ahead, the refueling stations may be required to conduct more frequent and rapid analysis and/or monitoring of the key impurity species, using simpler and inexpensive technologies. The device described here uses a novel impurity enrichment technique to allow the sample to be analyzed with simpler and less expensive analytical instruments. This paper describes this developmental device and presents test results demonstrating the feasibility of this concept.

2. Theoretical

2.1. The concept

A hydrogen selective metal membrane is at the core of this impurity enrichment method. Membranes made of metal-alloys, being extremely permeable to hydrogen but essentially impermeable to other gases, have been extensively studied and used for hydrogen purification [5–10]. The central function of hydrogen selective membranes is the presence of

a metal surface that dissociates and reassociates hydrogen molecules and transports atomic hydrogen through the bulk of the metal through a pressure gradient [6,7,10]. Hydrogen, being extremely soluble in metals such as Pd, is separated with high selectivity since the dense metal lattice prohibits the passage of other species (i.e. CO, CO₂, N₂).

The impurity enrichment is achieved by removing the hydrogen from the gas sample through a hydrogen selective membrane leaving the concentrated impurities in the enrichment vessel. Fig. 1 shows a schematic of the gas sampling and impurity enrichment device (GSIED). The device consists of two separately connected vessels – a high pressure rated sampling vessel and a lower pressure rated impurity enrichment vessel housing the hydrogen membrane. The GSIED will be connected to the nozzle of the dispensing stations, and after the requisite purging, collect the gas in the high pressure sampling vessel (vessel 1). The device will then be disconnected from the nozzle and taken to the laboratory for the “enrichment process”. This process, which is described in more detail in the next section, will consist of allowing the gas from the high pressure vessel to slowly flow into a lower pressure vessel housing the H₂-transport membrane (vessel 2). With hydrogen permeation, the pressure in the sampling vessel will decrease and when it reaches a low enough pressure, the flow between the two chambers will be stopped and the membrane will be cooled to stop the hydrogen permeation. Knowing the volumes (V₁, V₂) and the initial and final pressures of the respective vessels, it is possible to calculate the factor by which the concentration of the non-hydrogen species has been enriched.

Table 1 – SAE suggested guideline values for some impurities in hydrogen for fuel cell vehicles.

| Impurity ^a | Concentration (ppmv) |
|--|----------------------|
| Helium | 300 |
| Nitrogen (N ₂) + Argon (Ar) | 100 |
| Total Hydrocarbons – C1 Basis (HC) | 2 |
| Carbon Dioxide (CO ₂) | 2 |
| Carbon Monoxide (CO) | 0.2 |
| Ammonia (NH ₃) | 0.1 |
| Sulfur (S as H ₂ S, COS, etc) | 0.004 |

^a Hydrogen, minimum purity = 99.97%. Impurities excluding helium, must be <100 ppmv.

¹ For example, ASTM's D03 Work Item Nos. 4548, 6527, 8150, 6624, and 9211 are investigating the analysis of non-hydrogen constituents in hydrogen.

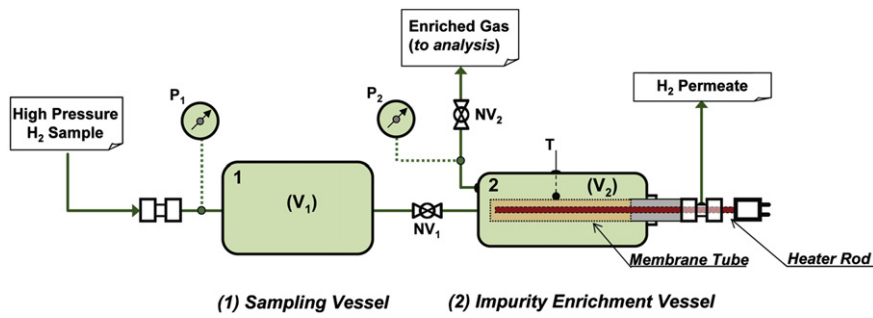


Fig. 1 – Schematic of the gas sampling and impurity enrichment device (GSIED).

2.2. Enrichment process and calculated enrichment factor (CEF)

Let us consider the enrichment process in more detail with the aid of Fig. 2, showing the GSIED during the enrichment process. Initially, step 0), the sampling vessel (vessel 1) and the impurity enrichment vessel (vessel 2) are purged at ambient conditions with the analyte gas containing hydrogen and trace amount of impurity species (i). The two vessels are isolated, and analyte gas is sampled at high pressure in the sampling vessel. Step a) defines the initial state of the gas mixture in the vessels after sampling. The total gas sample (n_T) is contained in the sampling vessel at a high pressure (P_{hi} , i.e. 6000 psig, ~410 atm) and at ambient pressure (P_{amb}) in the impurity enrichment vessel – analyte gas that remained after the initial purge.

In step b) the enrichment of the trace impurities in hydrogen begins. The gas is allowed to slowly flow from the sampling

vessel to the impurity enrichment vessel. As the temperature of the membrane (T_2) and pressure (P_2) in the enrichment vessel increases, hydrogen starts to permeate out through the membrane (at ambient pressure) enriching the concentration of the impurities in that vessel. The hydrogen permeation rate is a function of temperature and hydrogen pressure difference across the membrane. In most cases, at temperatures above 200 °C and for relatively thick membranes ($> \sim 5 \mu m$), the hydrogen flux is limited by the diffusion of hydrogen atoms through the metal membrane [6–8,10]. The hydrogen flux in such instances is described by Sievert’s law, and is proportional to the difference between the square roots of the hydrogen pressures on the two sides of the membrane [6]. Although a higher pressure differential will increase the hydrogen flux across the membrane and shorten the enrichment time, the allowable pressure in the impurity enrichment vessel (P_2) will be limited by the thickness and structural integrity of the membrane. As long as the pressure in the sampling vessel (P_1)

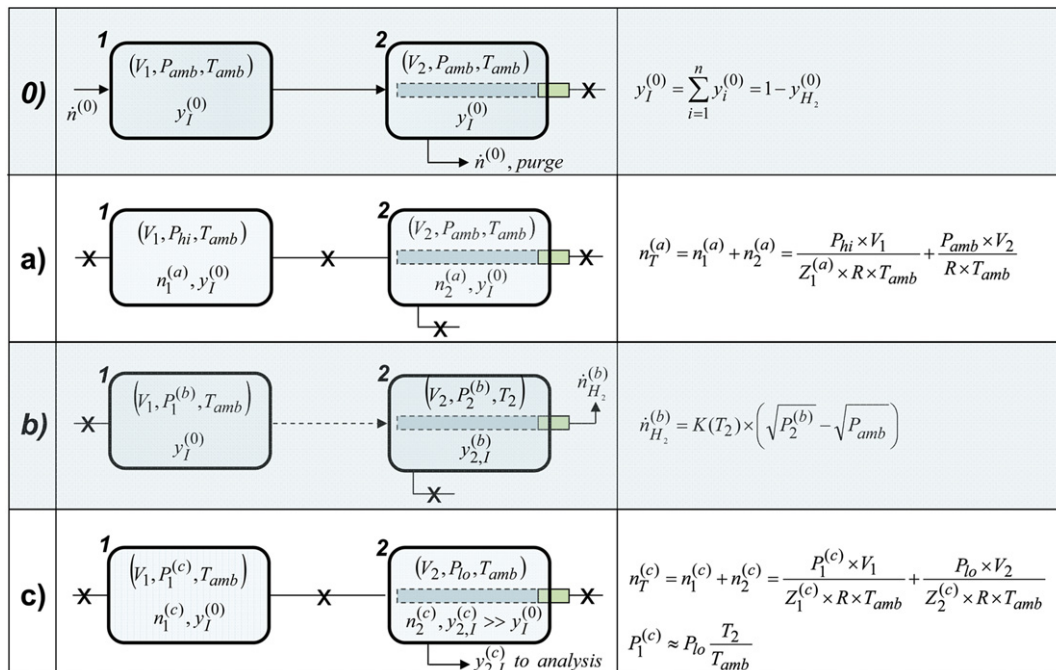


Fig. 2 – Steps of the sampling vessel (vessel 1) and impurity enrichment vessel (vessel 2) of the GSIED during the enrichment process. 0) Purge of the GSIED with analyte gas at ambient conditions, a) sample loading at high pressure (P_{hi}) and ambient temperature, b) H_2 permeation at elevated temperature in vessel 2, c) Cooling to ambient temperature and gas analysis at low pressure (P_{lo}).

is higher than the pressure in the impurity enrichment vessel (P_2), the flow of gas from the sampling vessel needs to be adjusted to match the hydrogen permeation rate. Alternatively, the impurity enrichment vessel can be periodically filled with gas to P_2 by opening and closing a valve connecting the two vessels. With time, as hydrogen leaves the system, the pressure in both vessels will be equal and approach ambient pressure. At low enough pressures, the flow between the two vessels is stopped and the membrane is cooled to ambient temperature, step c). At that point, the pressure in the enrichment vessel (P_{lo}) will be somewhat lower than the pressure in the sampling vessel (P_{hi}) due to the cooling process.

With hydrogen being the only species that permeates across the membrane, the total amount of impurities in the vessels during the initial sampling step (a) and final step (c) remain the same,

$$y_1^{(0)} \times n_T^{(a)} = y_{2,I}^{(c)} \times n_2^{(c)} + y_1^{(0)} \times n_1^{(c)} \quad (1)$$

and the enrichment factor, the molar fraction ratio of the enriched impurities to the impurities in the original gas, follows from Eq. (1),

$$\begin{aligned} \text{CEF} &= \frac{y_{2,I}^{(c)}}{y_1^{(0)}} = \frac{(n_T^{(a)} - n_1^{(c)})}{n_2^{(c)}} \\ &= \frac{\left(\frac{P_{hi} \times V_1}{Z_1^{(a)} \times R \times T_{amb}} + \frac{P_{amb} \times V_2}{R \times T_{amb}} \right) - \frac{P_1^{(c)} \times V_1}{Z_1^{(c)} \times R \times T_{amb}}}{\frac{P_{lo} \times V_2}{Z_2^{(c)} \times R \times T_{amb}}} \quad (2) \end{aligned}$$

The enrichment factor, which is illustrated in Fig. 3, is a function of the sample pressure, final pressure and the volume of the respective vessels. It shows that if the sample gas is collected at a dispensing pressure of the refueling station of 410 atm (~6000 psig), then a calculated enrichment factor as high as two orders of magnitude is easily achievable when the final pressure (P_{lo}) is reduced to 3 atm. It is notable that a reduction of the final pressure by half or doubling the vessel volume ratio leads to a near doubling of the enrichment factor. The calculated results² shown in Fig. 3 are based on the Peng–Robinson equation of state [11], however, assuming ideal gas behavior and extending $P_1^{(c)}$, this relationship is understood and can be appreciated by simplifying Eq. (2) as,

$$\text{CEF} \approx \left(\frac{P_{hi}}{P_{lo}} \times \frac{V_1}{V_2} \right) + \left(\frac{P_{amb}}{P_{lo}} \right) - \left(\frac{T_2}{T_{amb}} \times \frac{V_1}{V_2} \right) \quad (3)$$

Recognizing that the first term in Eq. (3) is the ratio of the molar mass in the sampling vessel at initial high sample loading pressure to the molar mass in the impurity enrichment vessel at a lower pressure, this term is at least an *order of magnitude* greater than 1, while the second and third terms are either slightly less than, or of the order of 1, respectively. Consequently, the enrichment factor is approximated to the ratio of the initial moles of gas in vessel 1 to the final moles of gas in vessel 2.

² For a high pressure process like this, the gas compressibility (Z) deviates from the ideal gas law and needs to be factored in to calculate the actual moles of gas being processed. Since the concentration of non-hydrogen species is very low, the compressibility of the gas can be approximated as for pure hydrogen.

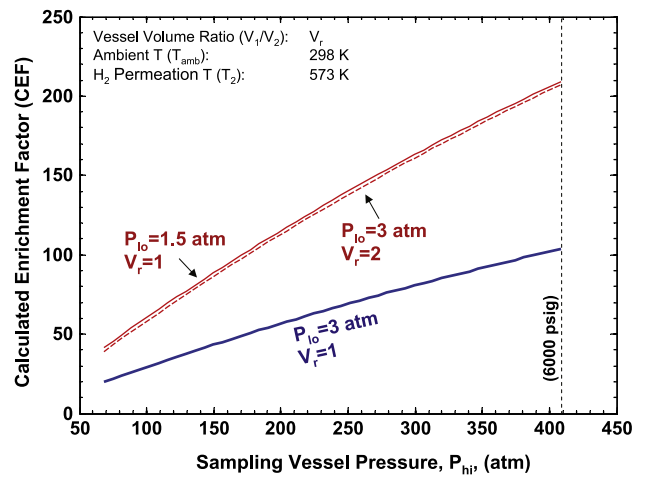


Fig. 3 – Calculated enrichment factor as function of the sampling and the impurity enrichment vessel pressures. Equation of state: Peng–Robinson [11].

Further, for identical vessel volumes ($V_1 = V_2$), the enrichment ratio reduces to the initial (high) to final (low) pressure ratio.

2.3. Concept challenges

To complete the enrichment within a reasonable time, it is necessary to raise the temperature of the membrane to achieve fast permeation. Elevated temperatures, however, raise the prospect of chemical reactions between the various species, such as methanation ($\text{CO} + 3\text{H}_2 \leftrightarrow \text{CH}_4 + \text{H}_2\text{O}$), water gas shift reaction ($\text{CO} + \text{H}_2\text{O} \leftrightarrow \text{CO}_2 + \text{H}_2$) and Boudouard reaction ($2\text{CO} \leftrightarrow \text{CO}_2 + \text{C}$), etc. Metal surfaces are known to catalyze many of these and other reactions. Considering that the impurity concentrations in the analyte gas are at trace levels, any reaction will lead to errors or variations between the calculated and measured enrichment factors. Similarly, the adsorption of species (e.g., sulfur species) on the interior walls of the hardware can also lead to variations between the measured and calculated enrichment factors.

The strategy for effective and predictable enrichment will depend on the ability to reduce these effects. This is achievable through a combination of (a) ensuring all wetted surfaces are inert or resistant to the adsorption of species such as sulfur, carbon monoxide, etc., (b) reducing the kinetics of the undesired reactions by lowering the temperature or the pressure of the enrichment chamber. Since lower temperature and/or pressure will reduce the hydrogen flux, this may require increasing the surface area of the membrane or allowing more time for the hydrogen permeation.

3. Experimental

3.1. Gas sampling and impurity enrichment device (GSIED)

Fig. 1 shows the schematic of the gas sampling device that was tested to demonstrate the concept and Fig. 4 shows a photograph of the hardware apparatus. The membrane sampling

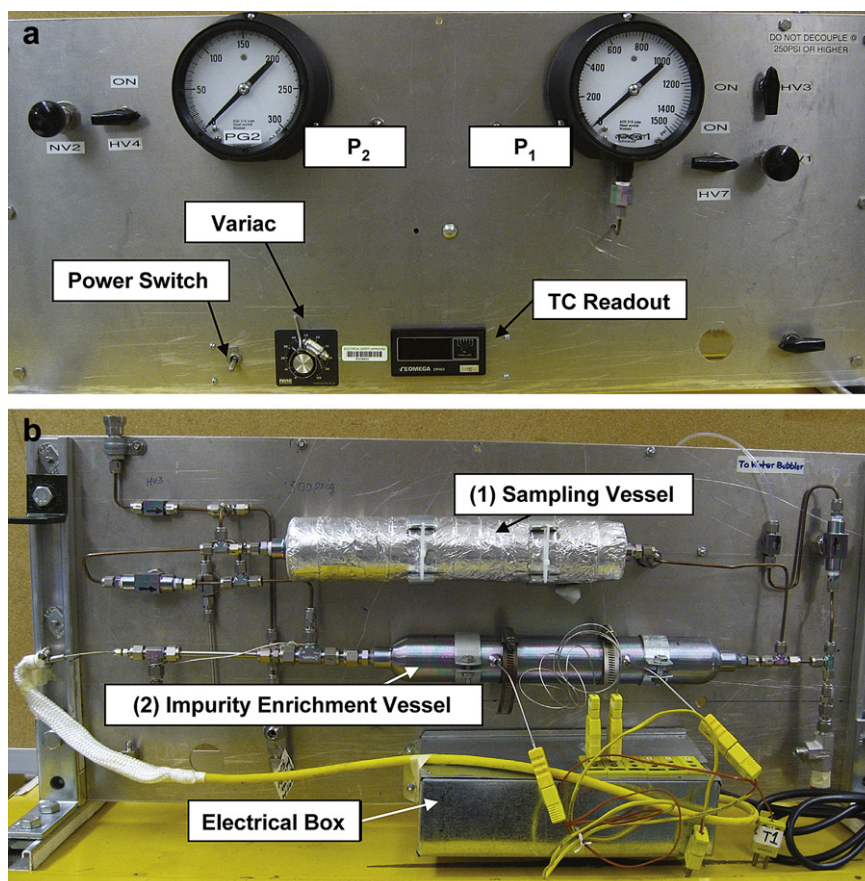


Fig. 4 – A photograph of the gas sampling and impurity enrichment device (GSIED). a) Front panel, b) Back panel.

device consists of a 500 cm³ sampling vessel (vessel 1) that is filled with the sample gas at high pressure, and a smaller 300 cm³ vessel (vessel 2) where the impurities are enriched. Vessel 1 is rated for service up to ~340 atm (5000 psig) at ambient temperature, while vessel 2 is rated for ~123 atm (1800 psig) and 400 °C and it is fitted with the hydrogen permeating membrane tube. The membrane tube is inserted within vessel 2 such that the permeate hydrogen can leave the system at ambient pressure. The membrane temperature is monitored with two thermocouples and is controlled with an electrical resistance heater rod inserted into the membrane tube. The pressures in the two vessels are monitored by separate pressure gauges (P₁ and P₂). Both vessels, tubes, and all fittings were internally passivated (SilcoNert™ 2000 coated by SilcoTek Corporation, Bellefonte, PA).

3.2. Membrane tube

The composition of the gases that the membrane will be exposed to is very important. Pd–Ag alloys, that otherwise show good performance for hydrogen permeability and durability, are susceptible to surface contamination [7]. For example, H₂S, even at ppm levels, strongly chemisorbs on the metal surface and may even form sulfides with the metal leading to a rapid decline in hydrogen permeability [12–15]. To maintain a reasonably high flux of hydrogen in the presence of H₂S, more sulfur resistant membranes must be used, i.e. alloying palladium with other metals such as copper or gold

[16–18]. Due to the presence of H₂S in some of the tests, a sulfur tolerant Pd/Cu-coated Pd–Ag alloy membrane tube was chosen for this development work³.

The membrane tube has dimensions of 4.76-mm-OD × 24.1-cm-long (0.187-in-OD × 9.5-in-long). The membrane is sealed at one end and brazed to a stainless steel tube at the other end. It is designed for operating conditions up to 300–350 °C and a pressure difference across the membrane of 20 atm (~300 psi).

3.3. Hydrogen gas

Two certified-grade hydrogen gas mixtures were obtained from Airgas Specialty Gases, LA. For our initial experimental tests (Series A) the hydrogen gas contained N₂, CH₄, CO, and CO₂ each at a concentration of 0.205%. To study sulfur enrichment, the second series of tests (Series B) was conducted with hydrogen gas containing 1000 ppmv each of N₂, CH₄ and CO₂, 100 ppmv CO, and 2.17 ppmv H₂S.

3.4. Analytical

The concentrations of H₂, N₂, CH₄, CO, and CO₂ were determined with a micro-gas chromatograph (Micro GC, Model M200H from Agilent Technologies, Inc., Wilmington, DE)

³ The membrane tube was provided by REB Research and Consulting, MI, USA.

equipped with thermal conductivity detectors. Two columns were used for the separation of the gases; a molecular sieve column was used for the separation of H₂, N₂, CH₄, and CO, and a 0.32-mm-ID × 6-m-long Poraplot-U column was used for the separation of CO₂ and higher hydrocarbons. For H₂S, an ASTM-approved (ASTM 4084-82) analyzer, based on the lead-acetate tape method, was used to measure the H₂S content in the hydrogen gas (Model 051 from Analytical Systems International KECO, Tomball, Texas). The concentrations of the sample gas determined by our analytical equipments were found to be within ±5% of the values certified by the gas supplier.

3.5. Experimental procedure

The experimental procedure consisted of

- Purging the apparatus with the analyte gas from the cylinder.
- Collecting the analyte gas sample (hydrogen with trace impurities) at an elevated pressure (P_{hi}) in the sampling vessel (vessel 1) in Fig. 1.
- Transferring the H₂ analyte gas from the sampling vessel to the impurity enrichment vessel (vessel 2) in Fig. 1.
- Heating the membrane tube to allow the hydrogen to permeate out through the membrane until the pressure in the sampling vessel was reduced to a desired lower pressure setting.
- Cooling the impurity enrichment vessel to ambient temperature and reading the final pressure (P_{fo}).
- Analyzing the gas remaining in the impurity enrichment vessel with analytical instruments.

At the end of the impurity enrichment process, the gas remaining in the impurity enrichment vessel is analyzed for the concentrations of the species. The experimentally measured enrichment factor (MEF) for each of the impurities is defined as,

$$MEF = \frac{C_{2,i}}{C_{0,i}} \quad (4)$$

where, $C_{0,i}$ is the measured concentration of impurity i in the original gas, and $C_{2,i}$ is the measured concentration of impurity i after enrichment in the impurity enrichment vessel (vessel 2).

Purging of the apparatus prior to sampling and enrichment of each new sample is an important part of the analytical process and should be conducted with the new gas to be sampled/analyzed. Since the apparatus includes flow space, dead-end spaces (lines to pressure gauges), and adsorption sites the vessels were purged by alternating between flow at ambient pressure (several multiples of the apparatus volume) and a pressure cycle. The latter consisted of pressurization and holding at 200 psig for 30 min, followed by depressurization. The effectiveness of the purge process was not studied systematically.

4. Results and discussion

The experimental work consisted of three sets: (1) tests to determine catalytic effects of the vessel surfaces at the enrichment conditions; (2) enrichment of impurities in

a sulfur-free hydrogen gas (series A); and (3) impurity enrichment in a sulfur-containing hydrogen gas (series B).

4.1. Effect of wall catalyzed reactions

The first set of tests was conducted to determine the extent of undesirable methanation and coking reactions that can take place on the vessel walls. The following are some reactions of concern.



The first test was conducted with a 316L stainless steel sample cylinder that was not passivated. The enrichment vessel (no membrane tube inside) was filled with the hydrogen gas (with impurities) at 14.6 atm (200 psig) and heated using an electrical coil wrapped around the exterior of the vessel. The external wall was heated to 350–400 °C and then maintained at that temperature for 3 h. The second test was conducted with a similar sized vessel, but one that was internally passivated with inert silicon coating (SilcoNert™ 2000). The enrichment vessel was again pressurized with the H₂ gas and heated up as before and held for 3 h. At the end of each test, the gas was analyzed for its impurity content.

Table 2 shows the results of the tests with and without the inert coating on the interior surfaces of the vessel. The vessel without silicon coating produced more CH₄ while the CO and CO₂ contents were reduced. Nickel and Ni–Fe alloys are well known catalysts for methanation of carbon oxides [19–21]. The Type 316L stainless steel vessel (consisting of 10–14% Ni, and 62–72% Fe) is believed to have catalyzed the observed methanation reactions of Eqs. (5) and (6) that occurred at the testing conditions. Eqs. (5) and (6) show that 1 mol of CH₄ is produced from each mole of CO or CO₂. However, Table 2 shows that an additional 0.16 mol of CH₄ was produced per

Table 2 – Effect of wall catalyzed reactions.

| Test conditions | 316L SS | 316L SS with Si coating |
|--|---------------|-------------------------|
| Pressure (atm) | 14.6 | 14.6 |
| Wall Temperature (°C) | 350–400 | 350–400 |
| Conc. [N ₂ , CH ₄ , CO, CO ₂] (Vol%) | 0.21 (±0.002) | 0.21 (±0.002) |
| Change in molar composition per mole of initial gas | (%) | (%) |
| N ₂ | –1 | +1 |
| CH ₄ | +16 | +1 |
| CO | –8 | +1 |
| CO ₂ | –19 | 0 |

mole of initial gas, but a total of 0.27 mol of CO and CO₂ were reduced, suggesting that some of the carbon oxides must have reacted to form coke via Eqs. (7) and (8). In contrast, the coated vessel maintained the species concentrations intact, as shown in Table 2. These test results confirm that the silicon coating is inert and it reduces or eliminates the undesirable methanation and coking reactions.

4.2. Initial tests without H₂S in the gas

The Series A tests were conducted with hydrogen that contained a relatively high concentration of the impurities, with ~0.21% each of N₂, CH₄, CO, and CO₂ as measured with our GC. Test conditions and results for two repeated tests are summarized in Table 3. Before each test, both vessels were purged with the analyte gas and the vessels were then isolated from each other by closing valve NV₁ (Fig. 1). Fig. 5 plots the membrane temperature, the pressures in the two vessels, and the calculated H₂ permeation (cumulative) during the test A-1 as example (the procedure for test A-2 was essentially identical to test A-1). The plots show three sections in time a), b), and c). In time section a), the experiment started out by pressurizing the sampling vessel (vessel 1) with the gas to an initial pressure (P₁) of 48.6 atm (700 psig) at ambient temperature. The pressure (P₂) in the impurity enrichment vessel (vessel 2) remained at 1 atm. The needle valve NV₁ between the two vessels was opened slightly to allow flow between the vessels and raise the pressure in vessel 2. At the same time, the heating element inside the membrane was powered-up to raise the surface temperature of the membrane to 220 °C. With increasing temperature, time section b), hydrogen began to permeate across the membrane eventually reaching a maximum permeation rate of ~120 ml/min at a pressure

differential of ~13 atm across the membrane. The pressure P₂ was maintained at ~14.6 atm by controlling the flow through NV₁ while the permeate side was kept at ambient pressure. The permeate stream was continuously analyzed in a gas chromatograph. No peaks corresponding to the impurity species present in the sample gas (i.e., N₂, CO, CO₂, CH₄) were detected, confirming the absence of pinholes in the membrane or leaks in the permeate gas lines.

As the pressure P₁ continued to decline it approached P₂ at approximately 150 min into the run. When P₁ reached 14.6 atm, NV₁ was fully opened and both P₁ and P₂ were observed to continue to decrease. When the pressure for both vessels reached the desired end point of 3.2 atm, at ~280 min, NV₁ was closed, the heating element was turned off, and vessel 2 was allowed to cool to room temperature reaching a final pressure of 2.3 atm (time section c). During the course of the enrichment, a total of ~20 L of hydrogen permeated out of vessel 2.

The impurities in the enriched gas in vessel 2 were then analyzed with a gas chromatograph, the concentrations of which are shown in Table 3. The measured enrichment factors (MEF), the ratios of the concentrations after and before enrichment, were calculated from Eq. (2). For the two repeated tests, the MEFs for N₂, CH₄, CO, and CO₂ were found to match the calculated enrichment factors (CEF), per Eq. (2). The initial and final concentration values used to calculate the MEFs in the table are averaged values from at least 5 analyses by gas chromatography, and the standard deviations indicate that the results were quite repeatable. The close match of the elemental material balance for N, C and O, also suggests very little loss (if any) of these species due to reaction or adsorption i.e., the errors were within the limits of uncertainty of the analytical equipment. The variation in the calculated

Table 3 – Test conditions and results of enrichment experiments without H₂S in the feed gas.

| Test Conditions/Results | Test A-1 | | Test A-2 | |
|--|---------------|---------------------------|---------------|---------------------------|
| Sampling Vessel (1) | | | | |
| Initial Pressure (atm) | 48.63 | | 48.63 | |
| Final Pressure (atm) | 3.22 | | 3.24 | |
| Conc. [N ₂ , CH ₄ , CO, CO ₂] (Vol%) | 0.21 (±0.002) | | 0.21 (±0.002) | |
| Impurity Enrichment Vessel (2) | | | | |
| Initial Pressure (atm) | 1 | | 1 | |
| Final Pressure (atm) | 2.31 | | 2.35 | |
| Membrane surface Temp. (°C) | 220 | | 220 | |
| ΔP Across Membrane (atm) | 12.9–13.6 | | 12.9–13.6 | |
| Final conc. (Vol-%) – N ₂ | 6.90 (±0.003) | | 6.82 (±0.006) | |
| Final conc. (Vol-%) – CH ₄ | 6.68 (±0.004) | | 6.63 (±0.005) | |
| Final conc. (Vol-%) – CO | 6.76 (±0.008) | | 6.73 (±0.017) | |
| Final conc. (Vol-%) – CO ₂ | 6.60 (±0.014) | | 6.54 (±0.008) | |
| Enrichment Factor (EF) | EF | Error relative to CEF (%) | EF | Error relative to CEF (%) |
| Calculated | 32.4 | | 31.8 | |
| Measured –N ₂ | 32.9 | +1.5 | 32.5 | + 2.2 |
| Measured –CH ₄ | 31.8 | –1.7 | 31.6 | –0.7 |
| Measured –CO | 32.2 | –0.5 | 32.0 | + 0.8 |
| Measured –CO ₂ | 31.4 | –2.9 | 31.1 | –2.0 |
| Elemental Material Balance (mol-%) | | | | |
| N | +1.5 | | + 2.2 | |
| C | –1.7 | | –0.6 | |
| O | –2.1 | | + 1.1 | |

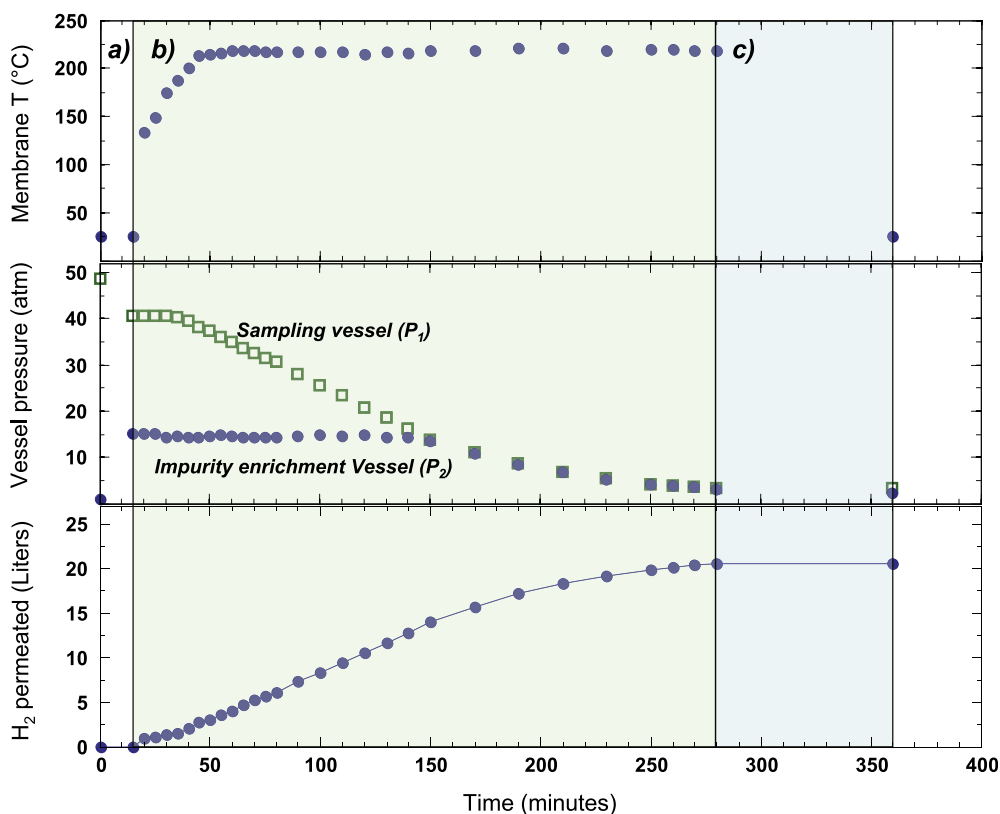


Fig. 5 – Plots of membrane temperature, pressure in both vessels and calculated rate (cumulative) of hydrogen permeation during the course of experiment A-1.

enrichment factors (32.4 and 31.8) between the two tests is due to the variability in the final pressures of the vessels.

Controlling the process manually required considerable care to ensure the same set-points as it affects the temperature and pressure history. The manual process involved adjusting a variac to maintain the membrane temperature, and NV_1 to maintain P_2 at ~ 14.6 atm.

4.3. Tests with hydrogen containing H_2S

One of the key impurities of concern in hydrogen for fuel cell vehicles is sulfur. The SAE guideline value (Table 1) for sulfur is 4 parts per billion (ppb). Such low concentrations being the driver for the development of this enrichment device, the next set of tests were conducted with hydrogen containing sulfur. The trace species in this gas included CO_2 , CH_4 , and N_2 at ~ 1000 ppm each, CO at ~ 100 ppm, and H_2S at ~ 2.2 ppm (see Section 3.3). These values were selected to be low enough to be considered “trace” yet high enough to be clearly quantifiable with our existing gas chromatograph and the lead-acetate detector.

Tests with the sulfur-containing gas (series B) started with an initial sampling vessel pressure (P_1) of 55.4 atm (800 psig) and the same test conditions as those described in the previous section (membrane tube temperature of 220 °C and differential pressure of ~ 13 atm across the membrane). The presence of sulfur reduced the membrane’s permeation rate quite sharply to ~ 13 ml/min, as compared to ~ 120 ml/min

observed in the tests without sulfur. This decrease in the hydrogen permeation rate indicates deactivation of the Pd/Cu-coated Pd–Ag alloy membrane by sulfur, possibly due to co-adsorbed H_2S and/or the formation of Pd and Cu sulfides, which would significantly reduce the hydrogen flux of the membrane [15].

By raising the membrane temperature, it was possible to partially recover the hydrogen flux. This effect of membrane temperature is shown in Fig. 6, where the cumulative permeation of hydrogen is compared at different temperatures. During the initial test (B-1) the membrane surface temperature was raised from 220 °C to 250 °C after 4 h into the run. The change in temperature affected the slope of the cumulative hydrogen permeation as the permeation rate increased from ~ 13 ml/min to ~ 40 ml/min. A second experiment (B-2) was conducted with the sulfur-containing gas with the membrane at 270 °C. The higher temperature accelerated the permeation still further, to ~ 65 – 70 ml/min. Even with this much higher membrane temperature, however, the presence of sulfur in the hydrogen extended the experiment time to nearly 6 h.

Table 4 summarizes the test conditions and analytical results for the tests with H_2S in the feed gas (B-1 and B-2). The calculated enrichment factor of 14.9–15.0 was lower than the ~ 32 in the previous tests without sulfur because we stopped this series of tests at a much higher final pressure than the previous tests (Table 3) so that more enriched gas sample would be available for sulfur analysis. Our analytical

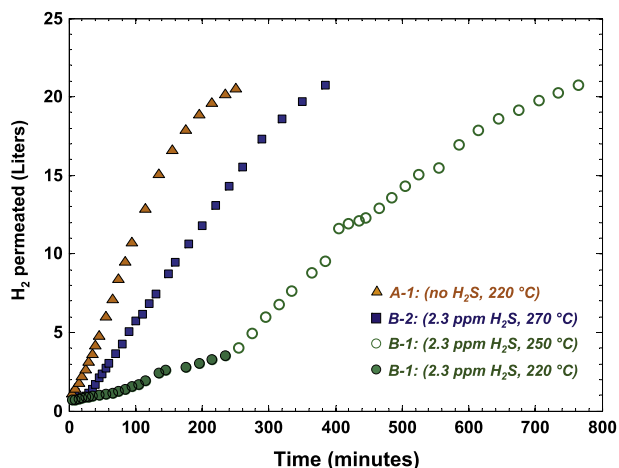


Fig. 6 – Effect of sulfur and membrane temperature on the permeation of hydrogen.

instrument to measure sulfur (lead-acetate tape method) required approximately 1–2 L of gas per analysis as opposed to a few mL of gas for GC-analysis. As in the previous tests, the measured enrichment factors (MEFs) for all non-sulfur species (N₂, CH₄, CO, and CO₂) matched well with the calculated enrichment factor (CEF). Again, the close match of the elemental material balance for the non-sulfur species also suggests very little loss of these species due to reaction or

adsorption, even at the membrane temperature of 270 °C. However, the measured enrichment factor for H₂S in the first test (B-1) was only 6.8, which was 55% lower than the calculated enrichment factor. After the second test, the enrichment factor for H₂S improved relative to the calculated enrichment factor, but there was still a 17% loss of the sulfur species. Since all the vessels, valves, and connecting tubes in the sampling device have been passivated with silicon coating, it is reasonable to believe that the observed loss of sulfur was due to the interaction of sulfur with the membrane tube.

If the chemical interactions between sulfur and the membrane tube are, indeed, the reason for the observed loss of sulfur, it is also reasonable to expect that the membrane tube will be gradually saturated by sulfur as more tests are conducted, and the loss of sulfur should gradually decrease and, eventually, stop. To investigate this hypothesis, a few more tests (B-3, 4, 5) were conducted under the same operating conditions as test B-2 (see Table 4). Fig. 7 summarizes the enrichment factors for all consecutive tests with H₂S in the feed gas (series B, 1–5). For the sulfur species, Fig. 7 shows that the MEFs increased with each successive test, reaching ~14 and leveling off after the third test (B-3). The MEFs for the non-sulfur species are again observed to match reasonably well with the CEF of 14.9–15. Within the limits of experimental and analytical errors, the analyses were quite repeatable for the non-sulfur species.

It should be noted that the certified sulfur content in the hydrogen gas is 2.17 ppm, but our H₂S analyzer (based on

Table 4 – Test conditions and results of enrichment experiments with H₂S in the feed gas.

| Test Conditions/Results | Test B-1 | | Test B-2 | |
|--------------------------------------|-------------|---------------------------|-------------|---------------------------|
| Sampling Vessel (1) | | | | |
| Initial Pressure (atm) | 55.4 | | 55.4 | |
| Final Pressure (atm) | 7.22 | | 7.72 | |
| Conc. (ppm) – N ₂ | 1010 (±45) | | 1010 (±45) | |
| Conc. (ppm) – CH ₄ | 1060 (±13) | | 1060 (±13) | |
| Conc. (ppm) – CO | 98 (±0.1) | | 98 (±0.1) | |
| Conc. (ppm) – CO ₂ | 1037 (±1) | | 1037 (±1) | |
| Conc. (ppm) – H ₂ S | 2.27 (±0.1) | | 2.27 (±0.1) | |
| Impurity Enrichment Vessel (2) | | | | |
| Initial Pressure (atm) | 1 | | 1 | |
| Final Pressure (atm) | 5.26 | | 5.23 | |
| Membrane surface Temp. (°C) | 220–250 | | 270 | |
| ΔP Across Membrane (atm) | 12.9–13.6 | | 12.9–13.6 | |
| Final conc. (ppm) – N ₂ | 15920 (±80) | | 15560 (±30) | |
| Final conc. (ppm) – CH ₄ | 15350 (±20) | | 15100 (±10) | |
| Final conc. (ppm) – CO | 1420 (±40) | | 1410 (±30) | |
| Final conc. (ppm) – CO ₂ | 15300 (±40) | | 15020 (±20) | |
| Final conc. (ppm) – H ₂ S | 15.38 | | 28.22 | |
| Enrichment Factor (EF) | EF | Error relative to CEF (%) | EF | Error relative to CEF (%) |
| Calculated | 15.0 | | 14.9 | |
| Measured – N ₂ | 15.8 | +5.2 | 15.4 | +3.3 |
| Measured – CH ₄ | 14.5 | -3.4 | 14.2 | -4.4 |
| Measured – CO | 14.5 | -3.3 | 14.4 | -3.5 |
| Measured – CO ₂ | 14.8 | -1.5 | 14.5 | -2.8 |
| Measured – H ₂ S | 6.8 | -54.8 | 12.4 | -16.6 |
| Elemental Material Balance (mol-%) | | | | |
| N | +5.2 | | +3.3 | |
| C | -2.5 | | -3.7 | |
| O | -1.6 | | -2.9 | |
| S | -54.8 | | -16.6 | |

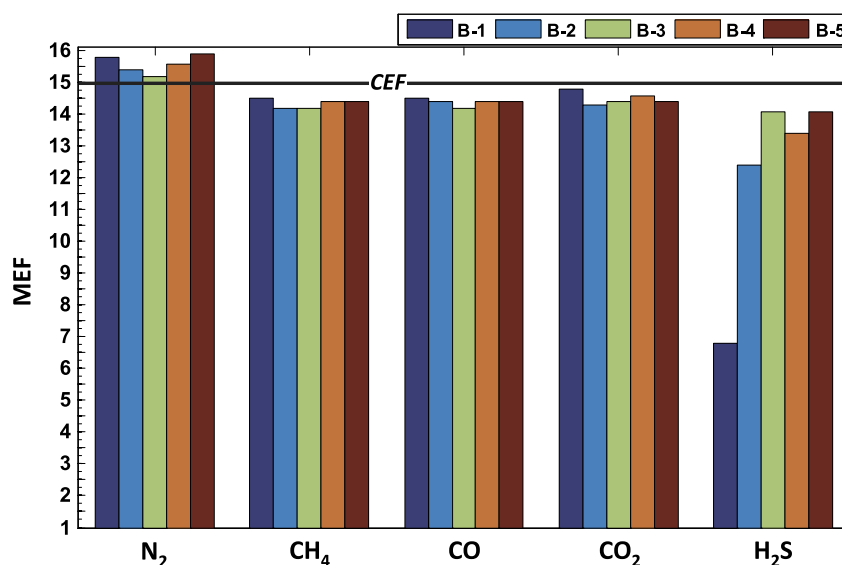


Fig. 7 – Enrichment factors for the consecutive tests B-1 to B-5.

lead-acetate sulfur sensing tape method) measured the H₂S in the feed gas to 2.27 ppm with a 5% margin of error. This analytical error may explain some of the observed sulfur loss in these tests. However, effects of the membrane temperature and the level of sulfur concentration on the extent of the sulfur uptake by the membrane tube and the possible reverse release of sulfur from the membrane tube are still not known, and more studies are needed to obtain a better understanding about these sulfur issues. The understanding of the sulfur loss mechanism, whether reacted or adsorbed on the membrane or any other surface is critical in order to develop appropriate solutions and test protocols.

4.4. Potential for field applications

The laboratory-scale sampling device reported in this paper can be further customized by appropriately packaging the vessels, piping, and the components to reduce the overall physical size of the device, and by maximizing the impurity enrichment factor through proper sizing of the two vessels.

Theoretically speaking the enrichment process depends only on the starting and end-points (pressure, temperature). In practice, controlling the temperature by adjusting a knob is difficult to reproduce at every experiment. Changes in the temperature/pressure history can change the extent of the side reactions, even if they are relatively small. Similarly, controlling the pressures to within 1 psig with a back-pressure regulator was found to be quite difficult in the laboratory, and thus automation should help repeat the starting and end-points better than can be achieved by human interface. A computer-driven automation of all control procedure steps to optimize its operation is desirable since it will achieve more repeatable control of the operational procedures, improve the analytical repeatability and reduce the total operation time. Through well designed customization and automation, this sampling device can effectively generate impurity-enriched samples that can be analyzed by simpler and less expensive

analytical techniques and equipments. Since the enrichment of this sampling device is a function of the sampler size and pressures in the chambers before and after enrichment, it can be easily tailored to achieve greater than two orders of magnitude for practical and economical field applications. Such a device can be deployed in the hydrogen production plants and fuel-cell vehicle refueling stations for the analysis and/or monitoring of key impurity species in hydrogen for quality assurance and control purposes.

5. Conclusions

A novel technique has been developed in this work to achieve a quantitative enrichment of trace impurities in hydrogen for allowing the enriched impurities in the sample to be analyzed with simple, low-cost analytical instruments in the field. A laboratory-scale sampling device using a Pd-alloy membrane has been designed, fabricated, and tested. In tests without sulfur impurities, the hydrogen analyte containing ~0.21% each of N₂, CH₄, CO, and CO₂ impurity species was sampled at 48.6 atm (700 psig) pressure and then processed in the device. The measured enrichment factors (MEFs) were found to match the calculated enrichment factors (CEFs) of ~32. The close correspondence between the MEFs and CEFs validates the concept of this sampling technique. The internal silicon coating of the wall surfaces of the sampling device has been shown to be effective in eliminating undesirable methanation and coking reactions, that otherwise may occur due to catalyzed reactions with the metal wall surfaces of vessel. Tests of the sampling device with hydrogen analyte containing ~2 ppm H₂S showed a reduction of hydrogen permeation rate as well as an initial sulfur loss. Test data showed the sulfur losses were reduced after a few consecutive tests, however, more studies are needed to address the mechanism of eventual sulfur loss and the initial sulfur accounting issues.

Acknowledgements

This work was supported by the U.S. Department of Energy's Vehicle Technologies and Fuel Cell Technologies Program Offices. Argonne National Laboratory is managed for the U.S. Department of Energy by UChicago Argonne, LLC, under contract DE-AC-02-06CH11357.

REFERENCES

- [1] Casey D, Verma P. Controlled hydrogen fleet and infrastructure demonstration and validation project, DOE hydrogen program review. Arlington, VA; June 2008.
- [2] Frenette G. Hydrogen fuel cell vehicle & infrastructure demonstration program review DOE hydrogen program review. Arlington, VA; June 2008.
- [3] Wipke K, Sprik S, Kurtz J, Thomas H, Garbak J. FCV learning demonstration: project midpoint status and first-generation vehicle results. *WEV J* 2008;2:4–17.
- [4] Information report on the development of a hydrogen quality guideline for fuel cells, SAE surface vehicle information report – J2719; Apr 2008. 1–14.
- [5] Basile A, Gallucci F, Paturzo L. A dense Pd/Ag membrane reactor for methanol steam reforming: experimental study. *Catal Today* 2005;104:244–50.
- [6] Baker RW. Membrane technology and applications. West Sussex: John Wiley & Sons; 2004. pp. 309–12.
- [7] Paglieri SN, Way JD. Innovations in palladium membrane research. *Sep Purif Methods* 2002;31:1–169.
- [8] Shu J, Grandjean BPA, Vanneste A, Kaliaguine S. Catalytic palladium-based membrane reactors – a review. *Can J Chem Eng* 1991;69:1036–60.
- [9] Knapton AG. Palladium alloys for hydrogen diffusion membranes. *Platinum Met Rev* 1977;21:44–50.
- [10] Phair JW, Donelson R. Developments and design of novel (non-palladium-based) metal membranes for hydrogen separation. *Ind Eng Chem Res* 2006;45:5657–74.
- [11] Poling BE, Prausnitz JM, O'Connell JP. The properties of gases and liquids. 5th ed. New York: McGraw-Hill; 2001. pp. 4.17–4.21.
- [12] Kajiwarara M, Uemiyama S, Kojima T. Stability and hydrogen permeation behavior of supported platinum membranes in presence of hydrogen sulfide. *Int J Hydrogen Energy* 1999;24:839–44.
- [13] Iyoha O, Enick R, Killmeyer R, Morreale B. The influence of hydrogen sulfide-to-hydrogen partial pressure ratio on the sulfidization of Pd and 70 mol% Pd–Cu membranes. *J Memb Sci* 2007;305:77–92.
- [14] Pomerantz N, Ma YH. Effect of H₂S on the performance and long-term stability of Pd/Cu membranes. *Ind Eng Chem Res* 2009;48:4030–9.
- [15] B.D. Morreale, The influence of H₂S on palladium–copper alloy membranes, Ph.D. thesis: University of Pittsburgh, School of Engineering, 2006. p. 156.
- [16] Morreale BD, Ciocco MV, Howard BH, Killmeyer RP, Cugini A, Enick RM. Effect of hydrogen-sulfide on the hydrogen permeance of palladium–copper alloys at elevated temperatures. *J Membr Sci* 2004;241:219–24.
- [17] Kamakoti P, Morreale BD, Ciocco MV, Howard BH, Killmeyer RP, Cugini AV, et al. Prediction of hydrogen flux through sulfur-tolerant binary alloy membranes. *Science* 2005;307:569–73.
- [18] Roa F, Thoen PM, Gade SK, Way JD, DeVoss S, Alptekin G. Palladium-copper and palladium-gold alloy composite membranes for hydrogen separations. In: Bose AC, editor. *Inorganic membranes for energy and environmental applications*. New York: Springer; 2009. p. 221–39.
- [19] Bustamante F, Enick RM, Killmeyer RP, Howard BH, Rothenberger KS, Cugini AV, et al. Uncatalyzed and wall-catalyzed forward water–gas shift reaction kinetics. *AIChE J* 2005;51:1440–54.
- [20] Kustov AL, Frey AM, Larsen KE, Johannessen T, Norskov JK, Christensen CH. CO methanation over supported bimetallic Ni–Fe catalysts: from computational studies towards catalyst optimization. *Appl Catal A* 2007;320:98–104.
- [21] Inui T, Funabiki M, Takegami Y. Simultaneous methanation of CO and CO₂ on supported Ni-based composite catalysts. *Ind Eng Chem Prod Res Dev* 1980;19:385–8.